

# Search for rotation in white dwarfs<sup>★</sup>

D. Koester<sup>1</sup>, S. Dreizler<sup>2</sup>, V. Weidemann<sup>1</sup>, and N.F. Allard<sup>3,4</sup>

<sup>1</sup> Institut für Theoretische Physik und Astrophysik der Christian-Albrechts-Universität, D-24098 Kiel, Germany

<sup>2</sup> Institut für Astronomie und Astrophysik, Waldhäuser Straße 64, D-72076 Tübingen, Germany

<sup>3</sup> Observatoire de Paris-Meudon, Département Atomes et Molécules en Astrophysique, F-92195 Meudon Principal Cedex

<sup>4</sup> CNRS Institut d'Astrophysique, 98 bis Boulevard Arago, F-75014 Paris, France

Received 2 June 1998 / Accepted 26 June 1998

**Abstract.** We report high-resolution spectroscopic observations of the NLTE  $H\alpha$  core in 28 DA white dwarfs. From a comparison with theoretically broadened NLTE models projected rotation velocities can be determined. The majority of objects are found to be compatible with zero or very small rotation with typical upper limits for  $v \sin i$  of 15 km/s, corresponding to periods of hours or longer. The implications for the loss of angular momentum during the evolution of the progenitors is discussed. Three new magnetic white dwarfs are detected with very small tangential fields in the range of 30 to 50 kG. In two more magnetic objects known before we found field strengths significantly larger than the mean longitudinal fields determined from the circular polarization. Very puzzling is the result for three ZZ Ceti stars in the sample, which all seem to have projected rotational velocities between 30 and 45 km/s, in conflict with asteroseismological results.

**Key words:** stars: white dwarfs – stars: rotation – stars: magnetic fields

## 1. Introduction

When Greenstein and Peterson (1973) detected the existence of sharp NLTE cores of  $H\alpha$  in white dwarfs of spectral type DA, which are characterized by otherwise strongly broadened Balmer lines, this opened the possibility to determine projected rotational velocities for these stars. This method has been applied through the years by several groups (Greenstein et al. 1977; Pilachowski and Milkey 1984, 1987; Koester and Herrero 1988) and most recently by Heber et al. (1997), who evaluated the Keck spectra obtained by Reid (1996) for the determination of gravitational redshifts. It turned out that the rotational velocities of white dwarfs are much smaller than one expects if angular momentum in the progenitor cores were conserved during stellar evolution.

That much of the initial angular momentum of a star could be lost became clear as one learned about the existence of strong

mass loss towards the white dwarf stage from initial-final mass relations derived for white dwarfs in open clusters (Weidemann and Koester 1983; Koester and Reimers 1996). However, the mechanisms and time scales for angular momentum transport from the cores to the envelopes remained unclear. Considering especially the Hyades case, Weidemann (1977) had already concluded that outward angular momentum transport had to be very effective early in the evolution towards the giant stage in order to explain the low observed rotational velocities of white dwarfs. In the meantime the situation has been sharpened by further reduction of observational limits on projected rotation velocities derived from line cores (typically around 10 km/s). Observations of magnetic white dwarfs and asteroseismological measurements give even longer periods with typical values around one day, corresponding to velocities of less than 1 km/s. These very low rotation velocities can only be achieved if solid rotation prevails through all of the pre-white dwarf evolutionary stages (Villata 1992; Spruit 1998). Whereas original magnetic fields can fairly easily enforce solid rotation from the beginning, this is much more difficult to achieve by hydrodynamical phenomena like convection, circulation, turbulence etc. in view of the molecular weight barriers created during stellar evolution. The low observed rotation velocities of white dwarfs thus implied, as was first pointed out by Hardorp (1974), Weidemann (1977), and Greenstein et al. (1977) that the molecular weight discontinuities are not very effective barriers to angular momentum transport out of the cores of evolving stars, and that solid rotation is enforced early after the main sequence, before the giant stages with their compact cores and very extended thin envelopes makes coupling much more difficult.

The theory of stellar evolution with angular momentum transport was developed and applied first by Endal and Sofia (1976, 1978, 1979). They calculated — under the assumption of rigidly rotating convection zones — the redistribution of angular momentum and chemical composition due to circulation currents in radiative layers by a diffusion technique. This has been taken over and developed in most recent studies, especially by the Yale group (Pinsonneault et al. 1989, 1990; Krishnamurthi et al. 1997).

Although their sophisticated approach, which includes pre-main sequence evolution and rotational braking by magnetic

---

Send offprint requests to: D. Koester

<sup>★</sup> Based on observations collected at the European Southern Observatory, La Silla, Chile (55.D-0459, 57.D-0631)

**Table 1.** Observed white dwarfs and atmospheric parameters. The abbreviations for the references are:

BR95: Bragaglia et al. (1995); B89: Bergeron et al. (1989); V97: Vauclair et al. (1997); SS94: Schmidt & Smith (1994); KV97: Koester & Vauclair (1997); BSL92: Bergeron et al. (1992); FKB97: Finley et al. (1997); BLF95: Bergeron et al. (1995a); KEP95: Kepler et al. (1995); B95: Bergeron et al. (1995b); KA93: Koester & Allard (1993); K97: Koester et al. (1997); UBv: determined from UBv colors for this paper

WD	name	$T_{\text{eff}}$	$\log g$	Ref
0047-524	L219-48	18750	7.83	BR95
0135-052	G271-115	7470	7.80	B89
		6920	7.89	binary
0310-688	LB3303	15700	8.16	V97
1350-090	LP907-037	9500	8.79	SS94
1422+095	GD165	11950	7.87	KV97
1425-811	L19-2	12200	7.99	KV97
1531-022	GD185	18850	8.39	BSL92
1544-377	L481-60	11250	8.09	V97
1615-154	G153-41	29600	7.95	FKB97
1620-391	CD-38° 10980	24250	8.05	V97
1743-132	G154-B5B	13950	7.71	BLF95
1827-106	G155-19	13800	7.61	KEP95
1840-111	G155-34	10230	8.18	KEP95
1919+145	GD219	14600	8.09	B95
1943+163	G142-50	19400	7.80	BSL92
1953-011	G92-40	7950	8.41	BR95
2007-219	L710-30	10000	8.18	BR95
2007-303	LTT7987	15150	7.86	BR95
2014-575	L210-114	26850	7.80	FKB97
2032+248	W1346	19900	7.87	V97
2039-202	L711-10	19350	7.95	V97
2039-682	L116-79	16050	8.44	BR95
2105-820	L24-52	10760	8.25	KA93
2115-560	L212-19	9950	8.13	BR95
2149+021	G93-48	17650	7.99	V97
2326+049	G29-38	11600	8.05	K97
2329-291	GD1669	24000	8.00	UBv:
2359-434	L362-81	8850	8.57	KA93

stellar winds, succeeds fairly well in reproducing the observed data on the evolution of rotational velocities and lithium abundances of young stars in open clusters (as a function of mass and age), they conclude that differential rotation survives in the cores of main sequence stars. The measured white dwarf rotational velocities of Pilachowski and Milkey (1987) of 20 km/s for 6 out of 20 observed white dwarfs are taken as argument in favor of their result, since a solid-body rotating model of the sun would predict a surface rotation velocity of 5 km/s if angular momentum is conserved locally and of only 1 km/s if solid rotation would be required through all of the pre-white dwarf AGB evolution.

An even stronger argument for differentially rotating cores after the main sequence is brought forward in the subsequent study of halo stars: Pinsonneault et al. (1991) demonstrate that the comparatively rapid rotation of horizontal branch stars, of the order of 15 km/s, as observed by Peterson (1983, 1985a,b),

can only be understood as a consequence of mass loss on the first giant branch, which uncovers the faster rotating deeper layers. They rule out rigid rotation enforced on a short time scale and thus oppose the assumption of strong coupling by a magnetic field (see however Spruit, 1998). The Yale group did not continue their actual evolutionary calculations through the RGB and horizontal branch and thus their conclusions were partly indirect, and point out the importance of better observations of rotational velocities for giants and white dwarfs. Rotational velocities for luminosity class III giants and subgiants of class IV have been listed and evaluated by Schrijver and Pols (1993) under assumptions about magnetic braking (with dynamo-action tied to convection). They conclude that subgiants (typically  $1.5 M_{\odot}$ ) have lost most of their angular momentum prior to reaching the RGB, while giants of class III (about  $2.5 M_{\odot}$ ) have lost about 50%, and that the exchange of angular momentum between radiative interior and convective envelope occurs on a time scale short compared to the angular momentum loss time scale by the magnetic wind. In the meantime better determinations for giants and subgiants have been obtained by CORAVEL measurements (De Medeiros et al. 1996a,b, 1997) which have not yet been evaluated.

Even in the case of the sun it is not yet known if the sun has a faster rotating core, as predicted by theoretical investigations (Endal and Sofia 1981, Pinsonneault et al. 1989), or is rotating rigidly. The results from seismological studies are still rather uncertain (e.g. Toutain & Kosovichev 1994), but seem to favor rigid rotation. Loudagh et al. (1993) give an upper limit of 6 times the average surface angular velocity, whereas Toutain & Kosovichev (1994) and very recently Charbonneau et al. (1998) find better agreement with the observations for rigid (slow) rotation of the core. Thus the question of the existence and the survival of differential rotation in stellar cores and thereby the prediction of white dwarf rotational velocities is still not solved. Evidently further observations are necessary in order to constrain the theoretical models. To do this in the white dwarf case is the purpose of the present study.

## 2. Observations

The observations for 28 southern DA white dwarfs were obtained in two runs from July 10 - 13, 1995, and July 26 - 29, 1996 at the La Silla observatory of the European Southern Observatory. The instrument used was CASPEC (Cassegrain ESO Echelle Spectrograph) at the 3.6 m telescope used in long-slit mode with an interference filter, giving a useful spectral range of about  $40 \text{ \AA}$  centered on  $H\alpha$ . The spectral resolution was  $0.26 \text{ \AA}$  as determined from the widths of Thorium lines in the comparison spectra. The detector was a TEK 1024x1024 CCD (ESO #37). Standard reduction techniques for flat-fielding, bias correction, extraction and wavelength calibration of one-dimensional spectra were applied using the procedures within IRAF. The final correction for the blaze function of the echelle was achieved very efficiently using a smoothed flatfield exposure.

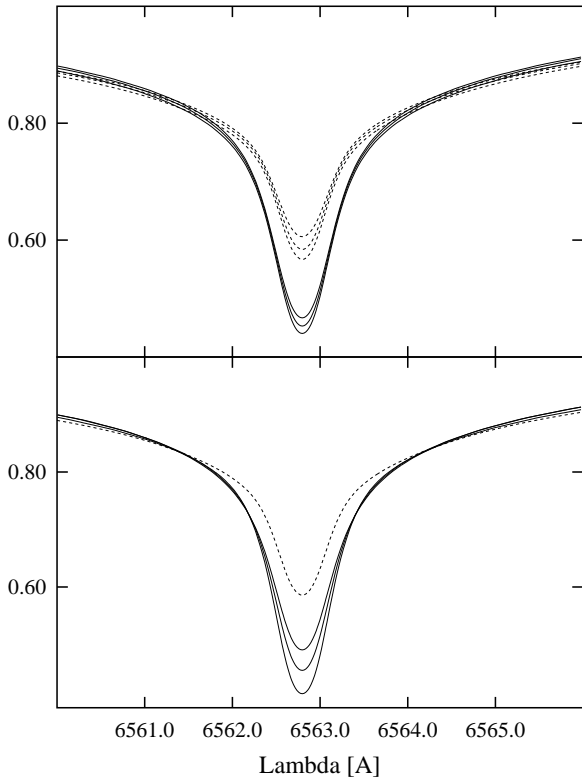


**Fig. 1.** Effect of  $T_{\text{eff}}$  (upper panel) and  $\log g$  (lower panel) on the depth of the NLTE core. All profiles have been normalized at 6552 and 6572 Å, similar to the procedure used for the comparison with observations. Temperatures in the upper panel are 14000, 13000, 12000 K (deepest core), with  $\log g = 8$ . Continuous lines are the NLTE models, the dotted lines show the corresponding LTE spectra. The lower panel shows models at 13000 K, with  $\log g = 7.5$  (deepest core), 8.0, 8.5. The dotted line is the LTE profile at 13000 K,  $\log g = 8$

The targets were the brightest DA white dwarfs chosen from the catalogue of McCook & Sion (1987). Exposure times were usually 60 min, except for the very brightest objects. In many cases more than one spectrum (up to 4) were obtained to correct for cosmic ray hits and to improve the signal-to-noise ratio. Multiple exposures were especially taken, if the  $H\alpha$  core looked broader than expected in a non-rotating DA.

Table 1 lists the objects observed, together with literature references for the effective temperature and surface gravity. Since all these stars are rather bright, many of them have several determinations in the literature. We have usually taken the most recent reference, with some occasional bias towards our own work.

### 3. Theoretical atmosphere models and synthetic spectra

The origin of the sharp core of  $H\alpha$  in cool DA white dwarfs as a NLTE effect has been discussed already by Greenstein & Peterson (1973), Pilachowski & Milkey (1984, 1987), Milkey & Pilachowski (1985), Koester & Herrero (1988), and Heber et al. (1997). With the exception of the last work, all previous authors have used LTE models to determine the temperature-

pressure stratification of the atmosphere. With this stratification kept fixed the line formation is then calculated in NLTE, solving the rate equations for the occupation numbers at each depth. We follow here essentially the same procedure, because the Werner & Dreizler NLTE code used (Werner & Dreizler 1998) does not include convection, which becomes important at lower temperatures. It is mostly for this reason that Heber et al. (1997), who use the same NLTE code for *consistent* NLTE calculations, were confined to the analysis of DA hotter than 14000 K. These authors have also shown that the differences between both methods are negligible for  $T_{\text{eff}} \leq 25000$  K, which is confirmed by our own test calculations. The version of the mixing length theory used for the LTE model calculations was  $ML2/\alpha = 0.6$ , which gives an intermediate efficiency for the convective energy transport as found appropriate for white dwarfs by Koester et al. (1994) and Bergeron et al. (1995b).

On the other hand, it is very important to treat the line blanketing effects in the LTE models very carefully. In the temperature range considered here the strongest blanketing effect is due to the strong Lyman lines. However, because the cores of these lines originate in the very uppermost layers of the atmosphere, their effect is largest at  $\tau_{\text{Ross}} \leq 10^{-8}$ . The core of  $H\alpha$  in the line formation calculation is strongly influenced by the temperature gradient in the range  $\tau_{\text{Ross}} = 10^{-6} - 10^{-4}$ , which in turn is determined by the blanketing effect of  $H\alpha$  itself and especially its core. We have therefore treated the blanketing by the lower Balmer lines very carefully, using 10 or more wavelength points even to resolve the Doppler core of the Stark profile.

$H^-$  absorption is the dominant absorption mechanism in cool DA, but usually not included in NLTE codes. We have included this process as a “background” absorption, calculated in LTE approximation.

Our model grid ranges from  $T_{\text{eff}} = 7000$  to 25000 K in steps of 1000 K, with additional models at 30000 K, and  $\log g = 7.5, 8.0, 8.5$ . Since Heber et al. (1997) have discussed the dependence of the NLTE core on temperature and surface gravity with many figures for their range of higher temperatures, we show here only one figure for lower  $T_{\text{eff}}$  spectra around 13000 K (Fig. 1). The main purpose is to demonstrate the small change with a change of the parameters, which allowed e.g. Pilachowski & Milkey (1984) to use only 2 different temperature models for the whole range. A step of 1000 K or 0.5 in  $\log g$  results in differences in the core, which are hardly noticeable on the figure. Typical errors in the parameters (see Table 1) are about 20% of this ( $\approx 200$  K, 0.1). Such small errors can be neglected in the determination of rotation velocities.

### 4. Comparison with observations and determination of $v \sin i$

A possible rotation of the white dwarf would influence only the innermost deep and narrow core of the broad  $H\alpha$  line. In the theoretical models this is simulated by convolving the theoretical spectrum with the rotational broadening function (Unsöld 1955; Koester and Herrero 1988). We have determined the limb darkening coefficients necessary for this convolution from angle-

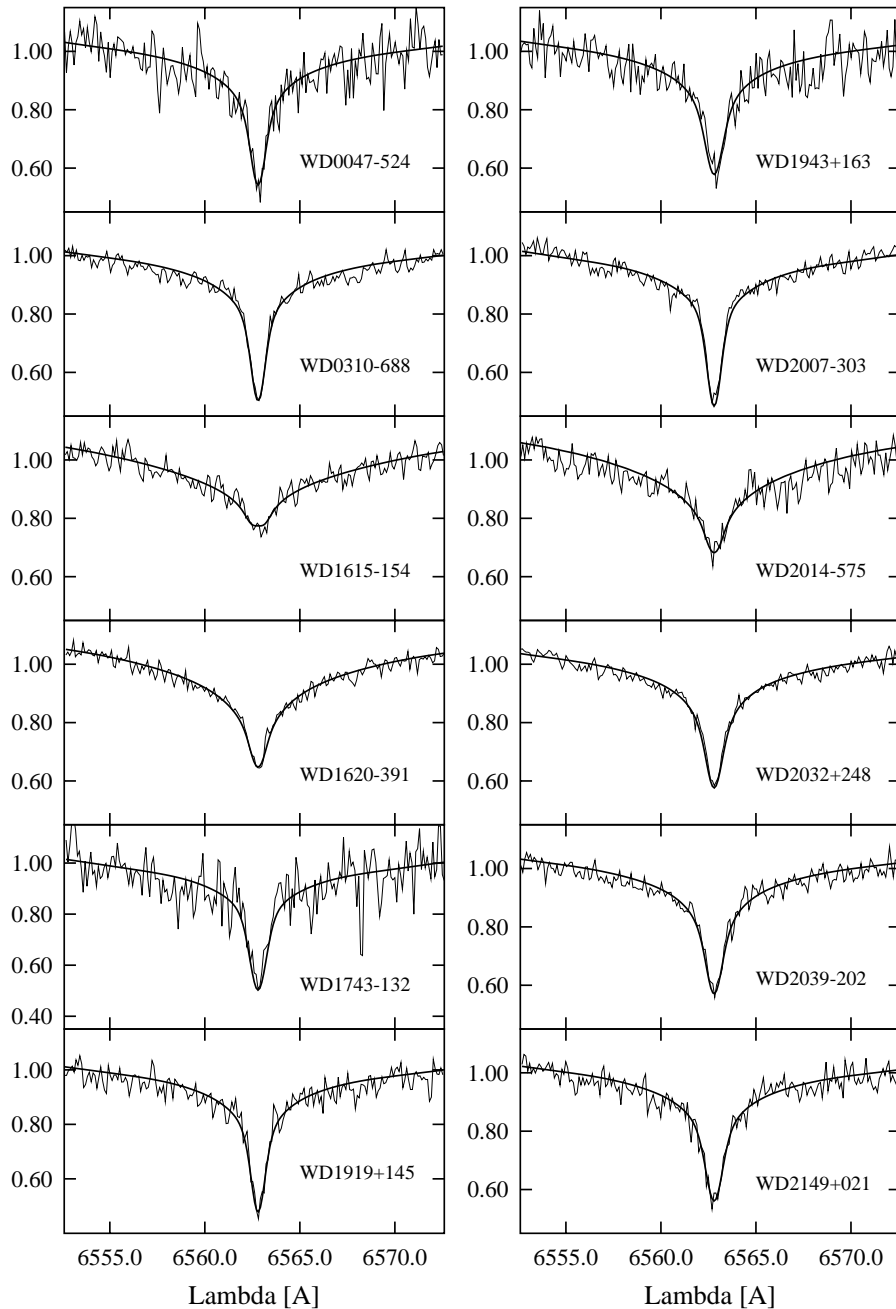


**Fig. 2.** Observed spectra (thin lines) and model fits for 12 DA with low rotation. See text.

dependent intensity calculations with the LTE code and found the linear coefficient in a  $20 \text{ \AA}$  interval around  $H\alpha$  to vary in the range 0.05 to 0.20, depending on temperature and distance from line center. Since a value below 0.5 has no influence on the resulting profile, we have continued to use 0.15 in all cases, as all authors have done before. After this convolution another convolution with a Gaussian of  $0.26 \text{ FWHM}$  takes into account the wavelength resolution of the observed spectra.

The determination of the best fit is done with a  $\chi^2$  method, using the amoeba routine (Press et al. 1992) to find the minimum. We have for this work preferred this method over the Levenberg-Marquardt method, which we normally use for spectral fitting, because it does not need derivatives and is very easily adapted

to different numbers of fit-parameters in arbitrary functions. In a first step we interpolate in our model grid for the correct  $T_{\text{eff}}$  and  $\log g$ . Then we use 3 free parameters to find the best fit of this model with zero rotation velocity to the spectral range  $6552$  to  $6572 \text{ \AA}$ . Free parameters are a scaling constant for the fluxes and a linear term to adjust the continuum slope, as well as a wavelength shift to adjust for a line-of-sight velocity or inaccurate wavelength calibration.

In a second step the theoretical profile is rotationally broadened and the best fit in a  $5 - 10 \text{ \AA}$  wide region around the core is determined, with the projected rotational velocity  $v \sin i$  as free parameter. When the minimum is found, we artificially increase the rotational velocity with all other parameters kept fixed, until

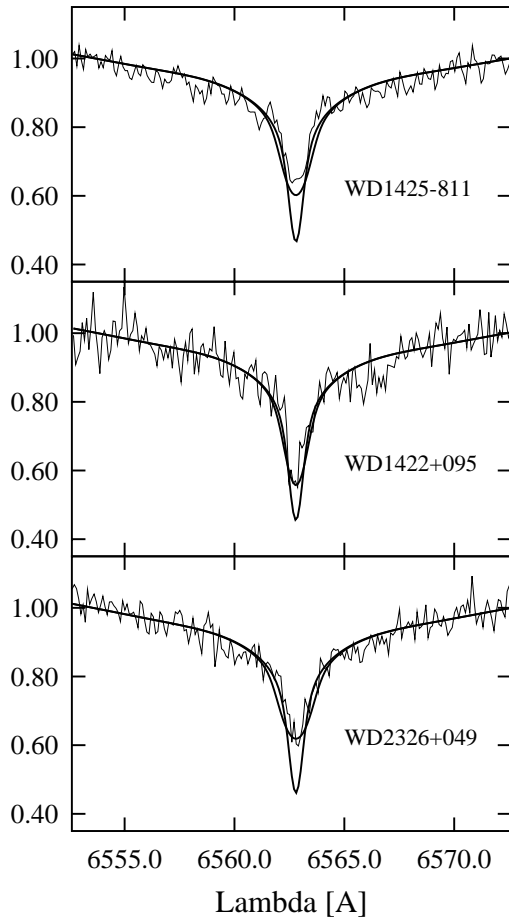


**Fig. 3.** Similar as Fig. 2, but for 3 ZZ Ceti stars in the sample with  $T_{\text{eff}}$  between 12200 and 11600 K. Thick lines are theoretical profiles with zero rotation (deeper core) and with the best-fit rotational velocity.

the  $\chi^2$  value increases over the minimum value by an amount corresponding to the  $1\sigma$  error (see Press et al. 1992, p. 660ff). This determines our error estimate for  $v \sin i$ , which therefore is a statistical error due to the noise in the data and does not include any systematic effects or uncertainties of the stellar parameters.

## 5. Results

With this paper we almost double the available number of spectroscopic determinations of projected rotation velocities, but the major result of the previous work does still hold up: white dwarfs are in general extremely slow rotators. Our results are summarized in Table 2 and will be discussed in several groups.

### 5.1. DA consistent with models with zero or very low $v \sin i$

Fig. 2 shows the fit for 12 DA (WD0047-524, WD0310-688, WD1615-154, WD1620-391, WD1743-132, WD1919+145, WD1943+163, WD2007-303, WD2014-575, WD2032+248, WD2039-202, WD2149+021), where the profiles are consistent with zero, or very small rotational velocities, obtained from a very good fit between models and observations.

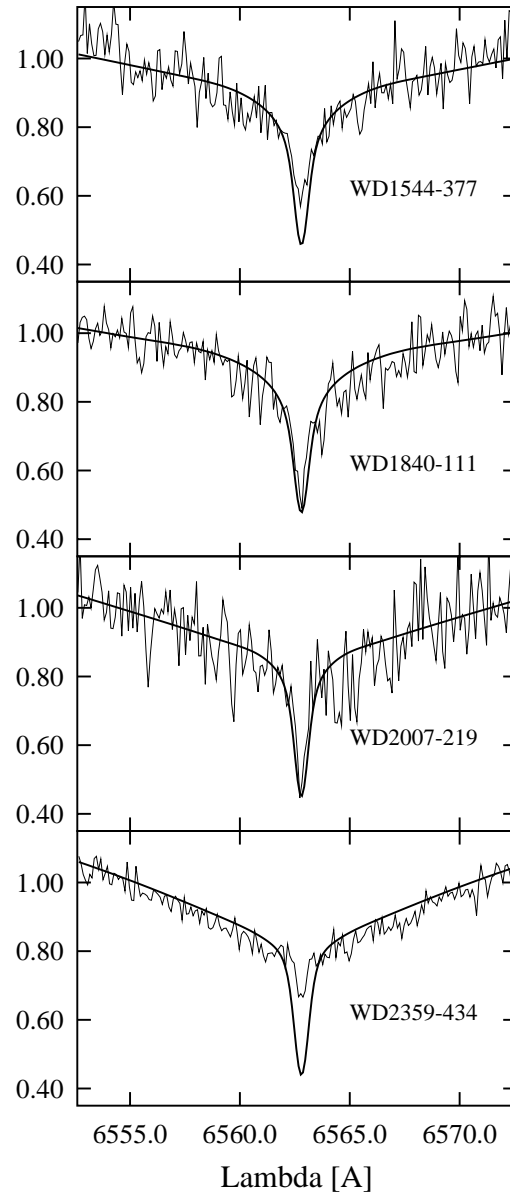


**Fig. 4.** Four DA with  $T_{\text{eff}}$  below the ZZ Ceti range (11250 - 8850 K).

In 7 out of 12 cases the best-fitting rotational velocity is compatible with 0 within the  $1\sigma$  error. For the remaining objects the result is only slightly larger (10 - 16 km/s). Considering possible systematic errors not included in our estimate (see previous section), we conclude that this whole sample of 12 objects is consistent with a population of non-rotating white dwarfs.

Since most of these spectra are consistent with unbroadened model spectra, we can also exclude any significant Zeeman splitting due to a magnetic field. Assuming very conservatively that a broadening of the core by  $0.4 \text{ \AA}$ , corresponding to almost 50%, would be easily recognized, we derive an upper limit for the field of 10 kG for the high S/N spectra, and about 20 kG for the spectra with larger noise.

Finally we note that all these objects are hotter than  $\approx 14000 \text{ K}$ .

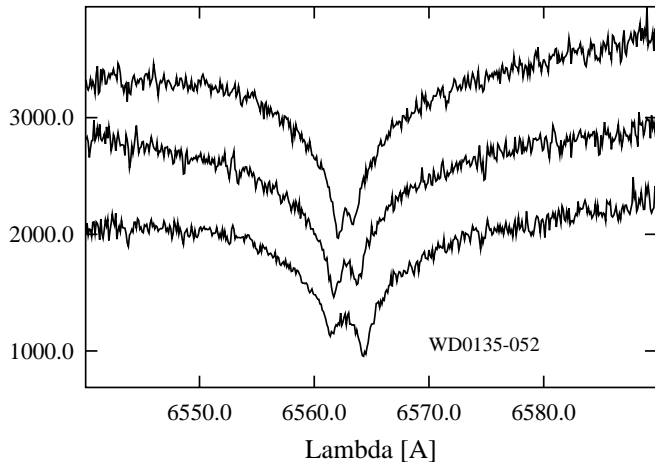


**Fig. 5.** Three spectra of the well studied binary WD0135-052 = L870-2, obtained on Jul 26, 27, 28 of 1996 (from top). The vertical scale is correct for the top spectrum. The others have been shifted downward for clarity.

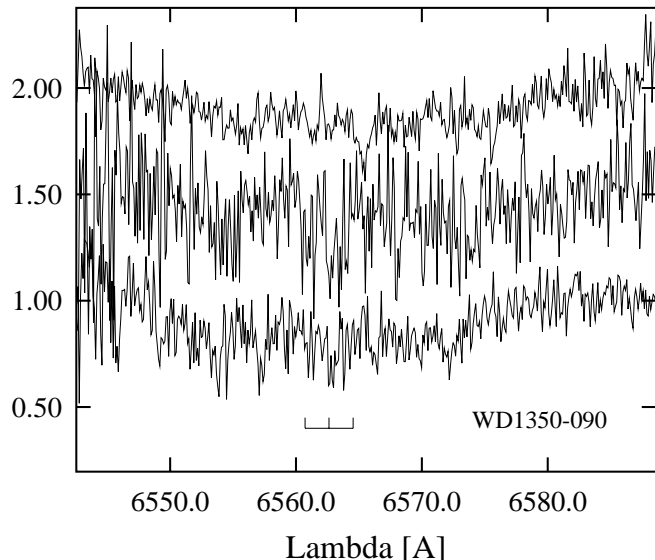


**Fig. 6.** Three spectra of the magnetic DA WD1350-090. The mark indicates the size of the Zeeman splitting expected from a 85 kG field as found by Schmidt & Smith (1994)

### 5.2. Line cores in ZZ Ceti stars

Fig. 3 shows a comparison similar to Fig. 2, but for the 3 ZZ Ceti stars in our sample (WD1428-811 = L19-2, WD1422+095 = GD165, WD2326+049 = G29-38) with  $T_{\text{eff}}$  from about 12200 K to 11600 K. In contrast to the hotter DA, in all of these objects the formal best fit is obtained with a significant rotational velocity of 30 to 45 km/s.

All objects have been studied extensively with asteroseismology, including observing campaigns with the Whole Earth Telescope (Kleinman et al. 1998; Sullivan 1995; O’Donoghue and Warner 1987; Bergeron et al. 1993). Multiplet splitting of frequencies is observed in all three, but the interpretation is difficult since the splitting is not always exactly equidistant. How-

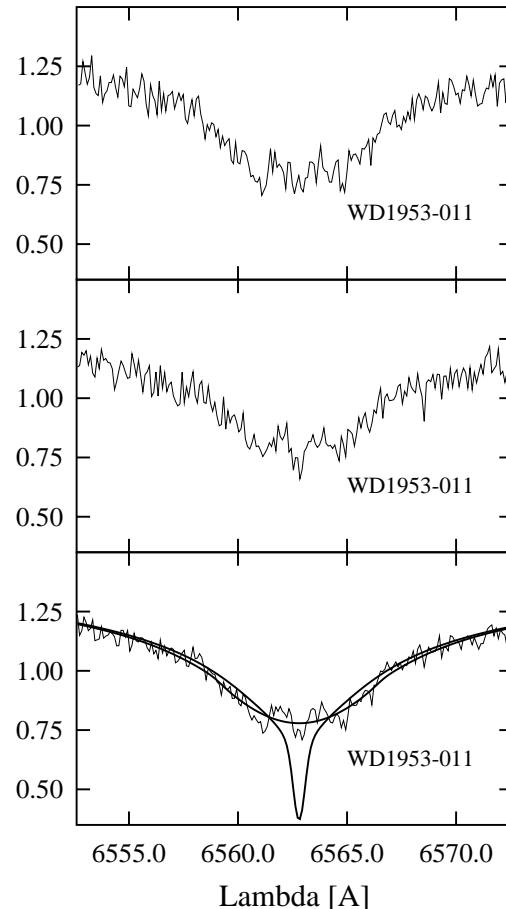


**Fig. 7.** Two independent spectra and the sum of both of the magnetic star WD1953-011. The lower panel with the sum spectrum also shows a model with zero rotation and one with  $v \sin i = 173$  km/s.

ever, all evidence from the size of the splitting points to rotation periods of the order of one day as in other variable white dwarfs, corresponding to rotational velocities below 1 km/s.

Non-radial oscillations in these objects should be associated with horizontal motion at the surface, which could in principle lead to line broadening similar to the rotation effect. Linear stability analysis cannot predict the amplitude of this oscillation. Assuming very crudely a shift of order 1% of the radius in one period, we find average velocities of less than 1 km/s. Similarly convection, at least according to the mixing length approximation used in our models, leads to velocity fields of the same order of magnitude, but does not even reach up in the atmosphere into the region, where the  $H\alpha$  core is formed. Hydrodynamical simulations of the Kiel group (Ludwig et al. 1994; Freytag 1998) show that the velocity fields reach up much higher in the atmosphere than predicted by the mixing length approximation. The vertical rms velocities at optical depth  $10^{-3}$  increase along the cooling track from below 1 km/s at  $T_{\text{eff}} = 13500$  K to about 6 km/s at 11500 K. But even these values are much too small to explain the observed profiles.

A close inspection of the fits with rotationally broadened profiles shows that the non-zero rotation is forced mostly by the

**Table 2.** Results of model fitting: rotation and magnetic fields. See text for a description of the derivation and of individual objects.

WD	$v \sin i$ [km/s]	B [kG]	remarks
0047-524	$1 \pm 11$	$< 10$	
0135-052			binary wd
0310-688	$0 \pm 4$	$< 10$	
1350-090		1000:	3 noisy spectra log $g = 8.79$
1422+095	$29 \pm 7$		ZZ Ceti
1425-811	$38 \pm 3$		ZZ Ceti
1531-022	$50 \pm 6$		log $g = 8.39$
		$35 \pm 16$	alternative narrow core
1544-377	$\approx 0$		
1615-154	$0 \pm 13$		
1620-391	$0 \pm 8$	$< 10$	
1743-132	$13 \pm 8$		
1827-106	$< 20$	$< 20$	very noisy
1840-111	$\approx 0$		narrow core
1919+145	$0 \pm 6$	$< 10$	
1943+163	$16 \pm 8$	$< 20$	
1953-011	$173 \pm 10$	$93 \pm 5$	log $g = 8.41$ narrow core
2007-219	$\approx 0$		
2007-303	$0 \pm 7$	$< 10$	
2014-575	$0 \pm 14$	$< 20$	
2032+248	$11 \pm 5$	$< 10$	
2039-202	$10 \pm 5$	$< 10$	
2039-682	$78 \pm 6$		log $g = 8.44$ alternative
		$\approx 50$	
2105-820	$65 \pm 5$	$43 \pm 10$	log $g = 8.25$
2115-560	$< 35$		noisy spectrum
2149+021	$16 \pm 5$	$< 10$	
2326+049	$45 \pm 5$		ZZ Ceti
2329-291	$26 \pm 4$	$31 \pm 10$	log $g = ?$
2359-434	$\approx 0$		very small core

relatively flat cores. Outside the cores ( $\approx \pm 1 \text{ \AA}$ ) the profiles are wider than the observed cores. This seems to indicate that our theoretical (zero-rotation) profiles are slightly too broad, and also makes improbable an explanation with magnetic fields, consistent with the findings of Schmidt and Smith (1995) for two of the objects.

There are major differences in the DA atmospheres for  $T_{\text{eff}}$  above and below about 14000 K: in the lower  $T_{\text{eff}}$  range the models become convective and  $\text{H}^-$  becomes the dominant source of opacity. We have carefully checked all aspects of the calculations, but were not able to find any reason, why our models should fail in this temperature range. We conclude that — if the low rotation of these objects is finally confirmed by asteroseismology — there must be an unidentified physical effect broadening the stellar spectra or leading to too broad and deep theoretical profiles.

### 5.3. The temperature range from 11500 to 8500 K

Fig. 4 shows 4 DA with  $T_{\text{eff}}$  below the ZZ Ceti range. WD1544-377 is with  $T_{\text{eff}} = 11250 \text{ K}$  still close to the instability strip and

shows a similar discrepancy between observation and theoretical profile. Even more than in the ZZ Ceti case it is clear here, that the theoretical profile is too broad and rotational broadening would not improve the fit. For the next two objects around 10000 K the fit with unbroadened profiles becomes satisfactory again, with the observation being only marginally broader than the model. We conclude that for these three objects our models do not fit perfectly, but that we can be confident that any rotation has to be very small.

Finally, in WD2359-434 (L362-81) at  $T_{\text{eff}} = 8850 \text{ K}$  the observed core is much smaller — narrower and flatter — than our zero-rotation model predicts. We have no explanation in this case and can only speculate, that perhaps we see only the unshifted component of a Zeeman triplet, with the other components shifted outside the observed spectral range or smeared out due to the inhomogeneity of the field. One argument in favor of this speculation could be the unusually high surface gravity of this object (see below).

### 5.4. Individual peculiar objects

WD0135-052: This object (= G271-115 = L870-2) was found to be a binary DA with a period of 1.56 days by Saffer et al. (1988). An analysis using all available constraints (Bergeron et al. 1989) resulted in the parameters for the two components given in Table 1. We obtain a better fit for our 3 spectra with effective temperatures higher by about 500 K; since we can use only the core of  $H\alpha$  our result cannot be compared to the much more careful analysis of Bergeron et al. (1989), but may indicate differences between the two atmosphere codes at the low-temperature end of the grid. We include the three spectra obtained in Fig. 5 as a demonstration that binaries with parameters similar to this pair could easily be detected by our technique.

WD1350-090: This DA was found to be magnetic by Schmidt & Smith (1994), who determined a disk-averaged longitudinal field of  $85 \pm 9 \text{ kG}$  from the circular polarization in  $H\alpha$  and  $H\beta$ . Fig. 6 shows the three spectra we have obtained. Although the quality is low, we do not see a splitting of the order of the triple mark (corresponding to a field of 85 kG), but instead a broad depression about  $20 \text{ \AA}$  wide. If this is caused by an inhomogeneous field, smearing out the core features, it would demand  $B \approx 1 \text{ MG}$ . Although the Zeeman splitting is sensitive to the average of the tangential component of the magnetic field instead of the longitudinal field in the case of polarimetry, such a large difference would be surprising. Moreover, from their low-resolution (unpolarized) flux spectrum Schmidt and Smith (1994) estimate an upper limit of 300 kG from the absence of detectable Zeeman splitting. Clearly this object deserves further study to confirm the magnetic field strength or any variability caused perhaps by rotation.

WD1953-011: Schmidt & Smith (1995) detected the lowest magnetic field so far ( $15.1 \pm 6.6 \text{ kG}$ ) in this object. Fig. 7 shows indeed a clear Zeeman triplet in two independent spectra and in the sum. The splitting, however, corresponds to a mean tangential field of  $93 \pm 5 \text{ kG}$ , again much larger than the longitudinal field found by Schmidt & Smith (1995). As shown in the figure,

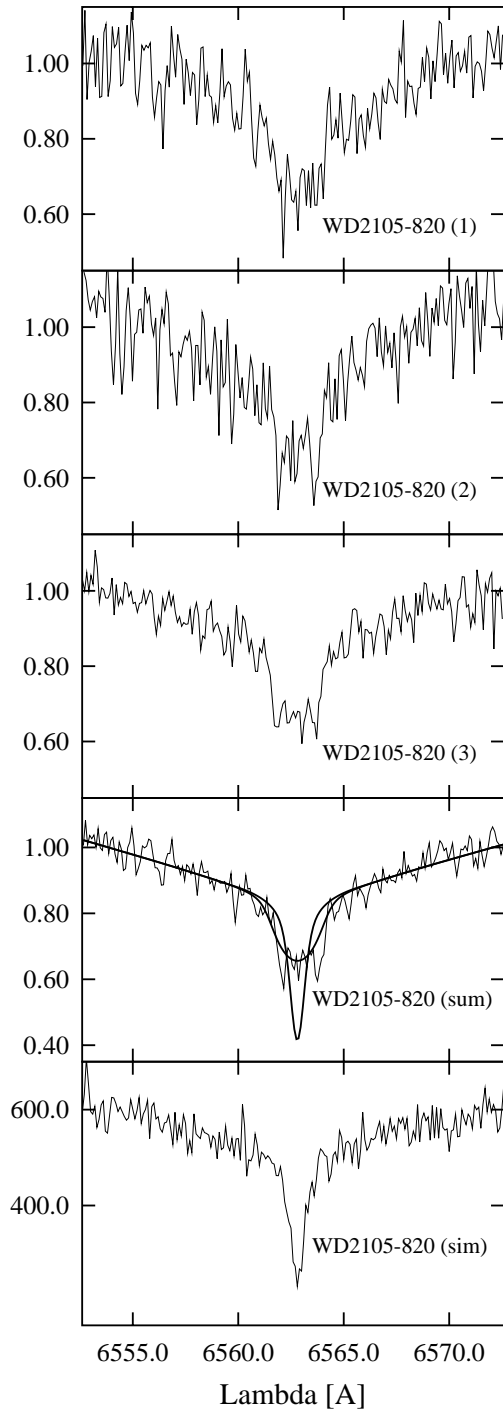


**Fig. 8.** Three independent spectra and the sum for WD2105-820. The fourth panel from top with the sum spectrum also shows a model with zero rotation and one with  $v \sin i = 63$  km/s, but the more plausible explanation is a magnetic field of 43 kG as discussed in the text. The lower panel is a simulation with realistic counts and noise sources.

a rotationally broadened spectrum with  $v \sin i = 173$  km/s would also give a reasonable fit. In this case, however, the clear triplet structure and the circular polarization provide clear evidence of a magnetic field.

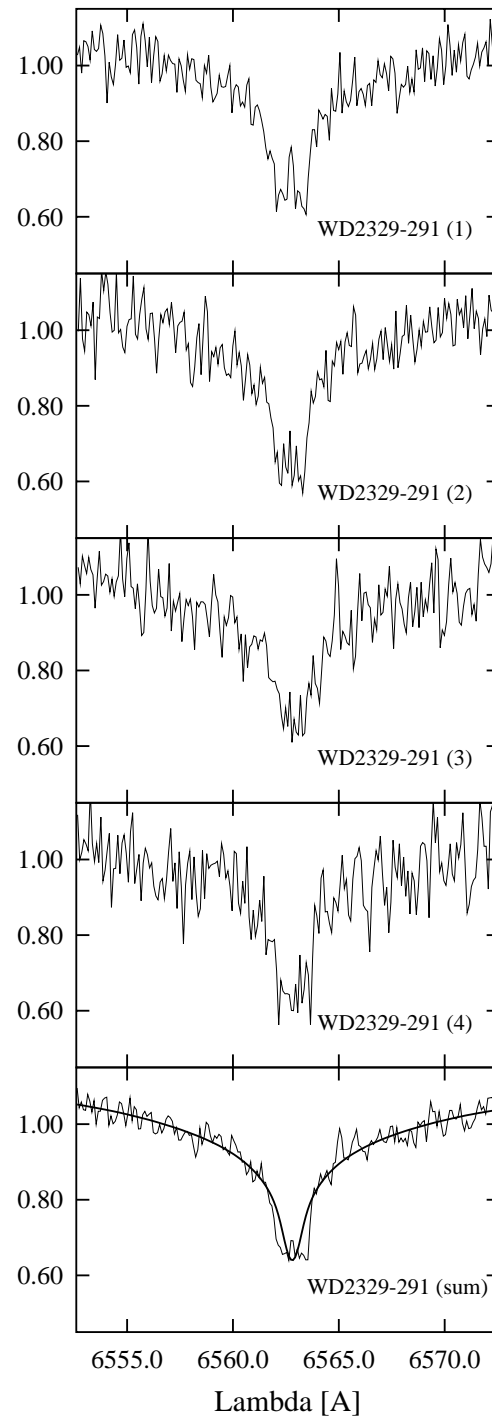


**Fig. 9.** Four individual spectra and the sum for WD2329-291. The bottom panel with the sum spectrum also shows a model with  $v \sin i = 26$  km/s, which does not fit at all. The plausible explanation is a magnetic field of 31 kG.

**WD2105-820:** This DA was not known to be magnetic before, but the three independent spectra in Fig. 8 clearly show the typical structure with flat bottom and individual components of a magnetic star, although the triplet structure is not as clear as in the previous object. The best fit resulting formally from rotational broadening is for  $v \sin i = 63$  km/s (4. panel from top).

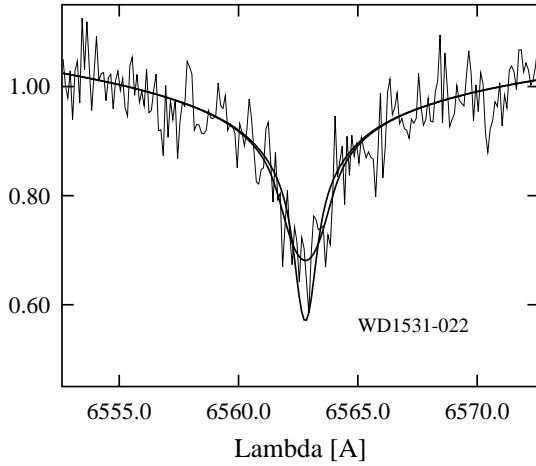


Fig. 10. Spectrum,  $v \sin i = 0$  and 50 km/s models for WD1531-022.

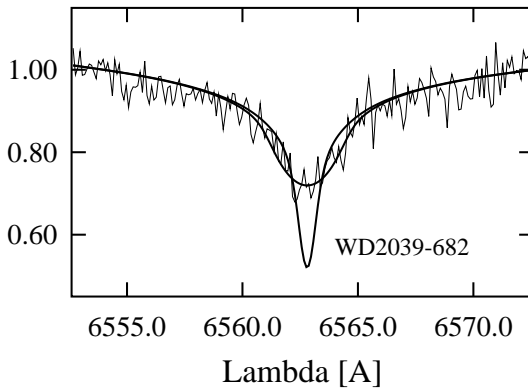


Fig. 11. Spectrum,  $v \sin i = 0$  and 80 km/s models for WD2039-682.

The fit is, however, unsatisfactory and a magnetic origin much more likely. We derive a field strength of  $43 \pm 10$  kG.

Since the S/N in these spectra is only about 20 or lower, and the flux is reduced in the line centers, we were concerned that such a flat bottom spectrum might be an artefact of a noisy spectrum. We have therefore simulated the observation as accurately as possible, starting from a model with correct parameters and adding noise due to all sources of noise known in the real observation and scaling to the correct level of the exposure. The result is shown in the bottom panel and demonstrates that the S/N in these observations is high enough to show the deep and narrow core if it were present.

WD2329-291: Almost nothing is known about this white dwarf and we had to determine the effective temperature of 24000 K from the UBV colors and a comparison with our theoretical grid, *assuming*  $\log g = 8$ . The core in four individual spectra (Fig. 9) clearly shows the broad, flat-bottom structure with several peaks, which we are by now convinced is indicating the Zeeman splitting in a magnetic field. The formal rotation solution with  $v \sin i = 26 \pm 4$  km/s is a totally unsatisfactory fit; we derive a magnetic field of  $31 \pm 10$  kG.

WD1531-022 and WD2039-682: both objects also show a broadened core, which, however, can be fit with rotationally broadened profiles of 50 and 80 km/s (Fig. 10 and Fig. 11.

Because of the shape of the core we favor a magnetic field of  $35 \pm 16$  kG as explanation for WD1531-022. Schmidt and Smith (1995) find an upper limit  $\leq 10$  kG from polarimetry, which may not be a contradiction regarding our result for WD1953-011. In the case of WD2039-682 an alternative explanation could be a magnetic field of  $\approx 50$  kG, but a distinction is not possible.

WD2115-560 and WD1827-106: the spectra for these objects have very low S/N. The sharp cores are clearly visible, but the upper limits derived (35 and 20 km/s) are not very stringent.

## 6. Discussion

Table 2 gives the final results for all objects discussed in the previous sections. The majority of results are compatible with zero rotation velocities, with typical upper limits of 10 - 20 km/s, corresponding to periods of the order of hours or longer. Of the exceptions, two were known before from polarization measurements to be magnetic (WD1350-090, WD1953-011). In both cases we find evidence for much larger fields than found by Schmidt & Smith (1994, 1995); one should, however, remember that the polarization measures the mean longitudinal field, whereas the Zeeman splitting indicates the average transversal field component over the stellar surface.

Three other objects are very likely new magnetic white dwarfs (WD2105-820, WD1531-022, WD2329-291) with magnetic fields between 30 and 50 kG. If these are confirmed, e.g. by measurements of circular polarization, it would indicate that the fraction of magnetic white dwarfs is significantly higher than the 4% estimated by Schmidt & Smith (1995). The observation of Zeeman splittings at high resolution requires a large telescope, but seems to be very efficient for the detection of small magnetic fields.

We note that of the five magnetic DA in this sample four have a surface gravity  $\log g \geq 8.3$ , and for the fifth object it is not known. If our speculation on WD2359-434 is correct (see above), this would add another high-gravity object to the magnetic class. We thus confirm the growing evidence for a correlation between white dwarf mass and magnetic field (Greenstein & Oke 1982; Liebert 1988; Sion et al. 1988; Schmidt et al. 1992; Schmidt & Smith 1994, 1995).

Only one single rotating object (WD2039-682,  $v \sin i = 80$  km/s) is remaining in the higher  $T_{\text{eff}}$  range, where our theoretical models have been proven to give very good fits to the observations. However, even in this case a magnetic field origin of the broadening cannot be excluded without circular polarization measurements.

A mystery remains the result for the ZZ Ceti in our sample. If taken at face value, the results indicate significant rotation with typical projected velocities of 30 - 40 km/s. It is hard to understand, how white dwarfs could acquire angular momentum, when entering the instability strip, and the result also seems to be in conflict with asteroseismological results. If this is confirmed, we will have to search for other broadening mechanisms in these objects, or for physical effects, which have been neglected in our theoretical models. For the time being we have no explanation; hopefully new observations of other members

**Table 3.** Spectroscopic determinations of rotation. A \* means that the rotation velocity is obtained formally, but that the more likely reason for the broadening is a magnetic field. See text and Table 2 for further explanations. \*\*: WD0205+250 was found to have a weak magnetic field by Schmidt & Smith (1994b). Codes for references are: PM84 Pilachowski & Milkey 1984; PM87 Pilachowski & Milkey 1987; MP85 Milkey & Pilachowski 1985; KH88 Koester & Herrero 1988; HNR97 Heber, Napiwotzki & Reid 1997

WD	$v \sin i$ [km/s]	reference	WD	$v \sin i$ [km/s]	reference
0047-524	$1 \pm 11$	this paper	1422+095	$29 \pm 7$	this paper
0205+250	$50 \pm 20^{**}$	PM87	1425-811	$38 \pm 3$	this paper
0310-688	$0 \pm 4$	this paper	1531-022	$50 \pm 6^*$	this paper
0326-278	$< 40$	KH88	1544-377	$\approx 0$	this paper
0352+096	$< 21$	HNR97		$30 \pm 20$	KH88
0401+250	$30 \pm 10$	PM87	1615-154	$0 \pm 13$	this paper
0406+169	$< 28$	HNR97	1620-391	$0 \pm 8$	this paper
0413-077	$< 20$	KH88		$< 20$	KH88
	$< 8$	HNR97	1659-531	$< 20$	KH88
	$< 19 \pm 5$	MP85	1716+020	$< 30$	KH88
	$10 \pm 10$	PM87	1743-132	$13 \pm 8$	this paper
0421+162	$< 18$	HNR97	1827-106	$< 20$	this paper
0425+168	$< 26$	HNR97	1840-111	$\approx 0$	this paper
	$10 \pm 20$	PM87	1911+135	$< 9$	HNR97
0431+125	$< 35$	HNR97	1919+145	$0 \pm 6$	this paper
0438+108	$< 28$	HNR97	1943+163	$16 \pm 8$	this paper
	$40 \pm 40$	PM87	1953-011	$173 \pm 10^*$	this paper
0644+375	$10 \pm 10$	PM87	2007-219	$\approx 0$	this paper
0726+393	$< 18$	HNR97	2007-303	$0 \pm 7$	this paper
0836+197	$< 43$	HNR97	2014-575	$0 \pm 14$	this paper
0837+199	$< 29$	HNR97	2032+248	$11 \pm 5$	this paper
0943+441	$< 32$	PM84		$10 \pm 10$	PM87
	$10 \pm 20$	MP85	2039-202	$10 \pm 5$	this paper
1104+602	$20 \pm 20$	PM84	2039-682	$78 \pm 6^*$	this paper
1105-048	$< 32$	PM84	2105-820	$65 \pm 5^*$	this paper
	$22 \pm 25$	MP85	2115-560	$< 35$	this paper
1134+300	$60 \pm 10$	PM84	2124+550	$40 \pm 40$	PM87
1137+321	$< 12$	HNR97	2126+734	$40 \pm 20$	PM87
1314+293	$< 29$	HNR97	2149+021	$16 \pm 5$	this paper
1327-083	$< 20$	KH88		$10 \pm 10$	PM87
	$< 44$	PM84	2326+049	$45 \pm 5$	this paper
	$42 \pm 9$	MP85	2329-291	$26 \pm 4^*$	this paper
1337+705	$30 \pm 20$	PM84	2359-434	$\approx 0$	this paper

of this class, or near this temperature range may shed more light on this problem.

In Table 3 we have for the convenience of the reader collected all spectroscopic determinations of rotation velocities known to us. Even considering the statistical uncertainty of the unknown inclination, there is now overwhelming evidence for extremely slow rotation of white dwarfs. Except for WD2039-682 and the ZZ Ceti stars mentioned above, where the result is somewhat doubtful, there is only one object (WD1134+300) left with  $v \sin i > 40$  km/s, which shows no evidence for magnetic field and has no conflicting second measurement. Being at rather high  $T_{\text{eff}}$ , the core is rather flat and this object should probably be reobserved and re-analyzed with modern model atmospheres. It should be remembered that Pilachowski & Milkey (1984) had only two model spectra available. At higher  $T_{\text{eff}}$ , where the absorption core becomes flat and finally goes over into an emission core, this may have influenced the result.

*Acknowledgements.* D.K. wants to thank Dr. L. Pasquini — then ESO staff member in La Silla — for his extremely valuable advice for the observations and interesting discussions.

## References

- Bergeron P., Fontaine G., Brassard P. et al. 1993, AJ, 106, 1987  
 Bergeron P., Liebert J., Fulbright M.S., 1995a, ApJ, 444, 810  
 Bergeron P., Saffer R.A., Liebert J., 1992, ApJ, 394, 228  
 Bergeron P., Wesemael F., Liebert J., Fontaine G., 1988, ApJ 345, L91  
 Bergeron P., Wesemael F., Fontaine G., Liebert J. 1989, ApJ, 345, L91  
 Bergeron P., Wesemael F., Lamontagne R., Fontaine G., Saffer R., Allard N.F., 1995b, ApJ, 449, 258  
 Bragaglia A., Renzini A., Bergeron P. 1995, ApJ, 443, 735  
 Charbonneau P., Tomczyk S., Schou J., Thompson M.J. 1998, ApJ, 496, 1015  
 De Medeiros J.R., Melo C.H.F., Mayor M. 1996a, A&A, 309, 465  
 De Medeiros J.R., Da Rocha C., Mayor M. 1996b, A&A, 314, 499  
 De Medeiros J.R., Do Nascimento J.D. Jr., Mayor M. 1997, A&A, 317, 701

- Endal A.S., Sofia S. 1976, *ApJ*, 210, 184  
Endal A.S., Sofia S. 1978, *ApJ*, 220, 279  
Endal A.S., Sofia S. 1979, *ApJ*, 232, 531  
Endal A.S., Sofia S. 1981, *ApJ*, 243, 625  
Finley D.S., Koester D., Basri G., 1997, *ApJ*, 488, 375  
Freytag B. 1998, priv. communication  
Greenstein J.L., Perterson D.M. 1973, *A&A*, 25, 29  
Greenstein J.L., Oke J.B. 1982, *ApJ*, 252, 285  
Greenstein J.L., Boksenberg A., Carswell R., Shortridge K. 1977, *ApJ*, 212, 186  
Hardorp J. 1974, *A&A*, 32, 133  
Heber U., Napiwotzki R., Reid I.N. 1997, *A&A*, 323, 819  
Kepler S.O., Giovannini O., Kanaan A., Wood M.A., Claver C.F. 1995, *Baltic Astr.*, 4, 157  
Kleinman S.J., Nather R.E., Winget D.E. et al. 1998, *ApJ*, 495, 424  
Koester D., Allard N.F. 1993, in "White Dwarfs: Advances in Observation and Theory", ed. M. A. Barstow, (Kluwer: Dordrecht), p. 237  
Koester D., Allard N.F., Vauclair G. 1994, *A&A*, 291, L9  
Koester D., Herrero A., 1988, *A&A*, 332, 910  
Koester D., Provencal J., Shipman H.L. 1997, *A&A*, 230, L57  
Koester D., Reimers D. 1996, *A&A*, 313, 810  
Koester D., Vauclair G. 1997, in "White Dwarfs", eds J. Isern, M. Hernanz & E. Garcia-Berro, (Kluwer: Dordrecht), p. 429  
Krishnamurthi A., Pinsonneault M.H., Barnes S., Sofia S. 1997, *ApJ*, 480, 303  
Liebert J.L. 1988, *PASP*, 100, 1302  
Loudagh S., Provost J., Berthomieu G. et al. 1993, *A&A*, 275, L25  
Ludwig H.-G., Jordan S., Steffen M. 1994, *A&A*, 284, 105  
McCook G.P., Sion E.M. 1987, *ApJS*, 65, 603  
Milkey R.W., Pilachowski C.A. 1985, *PASP*, 97, 634  
O'Donoghue D., Warner B. 1987, *MN*, 228, 949  
Peterson R.C. 1983, *ApJ*, 275, 737  
Peterson R.C. 1985a, *ApJ*, 294, L35  
Peterson R.C. 1985b, *ApJ*, 289, 320  
Pilachowski C.A., Milkey R.W. 1984, *PASP*, 96, 821  
Pilachowski C.A., Milkey R.W. 1987, *PASP*, 99, 836  
Pinsonneault M.H., Kawaler S.D., Sofia S., Demarque P. 1989, *ApJ*, 338, 424  
Pinsonneault M.H., Kawaler S.D., Demarque P. 1990, *ApJS*, 74, 501  
Pinsonneault M.H., Delyannis C., Demarque P. 1991, *ApJ*, 367, 239  
Press W.H., Teukolski S.A., Vetterling W.T., Flannery B.P. 1992, "Numerical Recipes" (Cambridge University Press: Cambridge)  
Reid I.N. 1996, *AJ*, 111, 2000  
Saffer R.A., Liebert J., Olszewski E.W. 1988, *ApJ*, 334, 947  
Schmidt G.D., Smith P.S. 1994, *ApJ*, 423, L63  
Schmidt G.D., Smith P.S. 1995, *ApJ*, 448, 305  
Schmidt G.D., Bergeron P., Liebert J., Saffer R.A. 1992, *ApJ*, 394, 603  
Schrijver C.J., Pols O.R. 1993, *A&A*, 278, 51  
Sion E., Fritz M.L., McMullin J.P., Lallo M.D. 1988, *AJ*, 96, 251  
Spruit H. 1998, preprint  
Sullivan D.J. 1995, *Baltic Astron.*, 261, 1995  
Toutain T., Kosovichev A.G. 1994, *A&A*, 284, 265  
Unsöld A., *Physik der Sternatmosphären* (Springer: Berlin), p.509  
Vauclair G., Schmidt H., Koester D., Allard N., 1997, *A&A* 325, 1055  
Villata M. 1992, *MN*, 257, 450  
Weidemann V. 1977, *A&A*, 59, 411  
Weidemann V., Koester D. 1983, *A&A*, 121, 77  
Werner K., Dreizler S. 1998, in *Computational Astrophysics, The Journal of Computational and Applied Mathematics*, eds. H. Riffert & K. Werner, Elsevier Press, Amsterdam, in press